https://ntrs.nasa.gov/search.jsp?R=19660002848 2020-03-24T03:41:29+00:00Z

NASA TECHNICAL MEMORANDUM

NASA TM X-1187

NASA TM X-1187

N66-12137
(ACCESSION NUMBER)
(THRU)
43
(PAGES)
1
(CODE)
(NASA CR OR TMX OR AD NUMBER)
32
(CATEGORY)
FACILITY FORM 602

GPO PRICE $
CFSTI PRICE(S) $
Hard copy (HC)
Microfiche (MF)

EVALUATION OF ONE TYPE OF FOLDABLE TUBE

by Laurence W. Gertsma, James H. Dunn, and Erwin E. Kempke, Jr.

Lewis Research Center
Cleveland, Ohio

NATIONAL AERONAUTICS AND SPACE ADMINISTRATION - WASHINGTON, D. C. - DECEMBER 1965

NASA TM X-1187

EVALUATION OF ONE TYPE OF FOLDABLE TUBE

By Laurence W. Gertsma, James H. Dunn, and Erwin E. Kempke, Jr.

Lewis Research Center
Cleveland, Ohio

NATIONAL AERONAUTICS AND SPACE ADMINISTRATION

For sale by the Clearinghouse for Federal Scientific and Technical Information
Springfield, Virginia 22151 – Price $1.00

EVALUATION OF ONE TYPE OF FOLDABLE TUBE

by Laurence W. Gertsma, James H. Dunn, and Erwin E. Kempke, Jr.

Lewis Research Center

SUMMARY

12137

Large space experiments present packaging problems at launch because of the limiting envelope of the launch vehicle. A "foldable tube" can be used to facilitate packaging by connecting components (i.e., radiators, nuclear reactors, etc.) with the system. When the tube is collapsed, it can be sharply bent or rolled into a coil for launch. Upon release of the holding mechanism in space, the tube will act as a self-erecting member for the component. After erection and self-expansion, the tube can be used to transport fluid or to act as a rigid structural member.

Three foldable-tube sections capable of transporting fluids when in the extended position were fabricated and tested. The design criterion of the tube is explained. The locations and directions of the maximum strains were determined by means of "Stresscoat," and the magnitude of the surface strain at these points was measured with strain gages. The maximum measured surface strain was near ±7000 microinches per inch. This investigation showed that such a tube can be fully collapsed and bent with a radius of curvature as small as 1.84 inches ($t/r = 0.011$ where t is the material thickness and r is the radius of curvature) without damage. Although any structural material can, in principle, be used, some especially suitable materials are the high-strength stainless steels, some nickel superalloys, titanium, and some hard copper alloys which have the large ratio of yield stress to modulus of elasticity desirable. This tube concept is suited for the positioning or extension of objects in space when structural strength or fluid-carrying capability is required.

Author

INTRODUCTION

Several power-generation systems for space use presently under study or development incorporate large fluid-carrying radiators to reject the waste heat from the system. The largest of these radiators must be compacted into a package size compatible with the launch vehicle and then erected when in orbit. The tube headers or supply lines will thus have to be hinged or broken in some manner to accomplish packaging.

There are often additional problems in packaging various spacecraft for launch in which the operating components need to be separated by a larger distance than that permitted by the envelope of the launch vehicle. This need requires an erection or extension of the components after rocket burnout by a device which will act as a structural member and in some cases as a fluid-carrying tube. When a nuclear reactor is used for power, for example, it is desirable to position it away from the vehicle to reduce the required size of the shadow shield.

Two techniques now in use for the extension of objects in orbit are the telescoping tube and the de Haviland tube. The de Haviland tube is essentially a split, thin-wall tube of a good springy material which is opened out flat and coiled for launch. When uncoiled, it reforms into a circular cross section, with the shape giving it rigidity. Both of these methods have their uses for the mere positioning of objects, but neither can act as a hot-fluid-carrying pipe in space, since the de Haviland tube is completely split longitudinally and the telescoping tube requires seals which have not been considered reliable for high-temperature liquids.

Several other methods both to extend an object and to have fluid-carrying capabilities could probably be developed, but they each have serious limitations. One method would be a joint with movable seals. This method is considered unacceptable because of the lack of seal reliability under adverse conditions. Failure of the seals in space would allow excessive loss of the working fluid, and failure on the ground would permit the working fluid to become contaminated by air leaking into the system.

Another method is to bend the tube itself into several loops and then partly uncoil them for erection. The elastic limit of the material and the large section modulus of a tube, however, permit only a small angle change per unit length. The tube therefore becomes quite long and heavy for a large angular deflection. The total pressure loss of the fluid would also tend to be large because of the long length, although the drop per unit length might be small.

A bellows is another approach to the problem, since it is flexible and reasonably light. It does have some serious problems though, such as the trapping of liquid in the convolutions. The convolutions would also cause a high frictional pressure drop since no internal sleeve could be used for large angular deflections. Because of its flexible characteristics, the bellows would be distended (perhaps broken) by the internal pressure unless longitudinal restraint is provided. Normally, for flexibility, very thin walls are used; this thinness could cause susceptibility to otherwise tolerable corrosion. The flexibility of either the bellows or the bent tube may require a structure to rigidify them after erection.

A solution to the sharp bending problem would be possible if the section modulus could be reduced. A tube configuration to replace short sections of the radiator headers is presented herein that permits reducing the section modulus to that of a thin plate by collapsing the section and thus permits the section to be bent as a flat plate without destructive yielding of the material. Upon release of a holding mechanism, in orbit, the "foldable tube" would deploy the radiator to the desired position and by self-expansion would snap into a fluid-carrying rigid structural member. The foldable tube could also be used to extend a nuclear reactor, with one end of each of two tubes rigidly attached to the vehicle structure and the other ends attached to the reactor. The reactor would then be rolled in the collapsed tubes and secured in the vehicle for launch. Prior to system startup the reactor would be deployed out from the vehicle by unrolling the reactor and tubes. The expanded tubes would then carry the reactor coolant to and from the vehicle.

The purpose of this initial investigation is to determine the practicability of such a foldable tube by fabrication of several specimens with different contours and by demonstration of their collapsing and bending capability. Selected strain measurements recorded during the collapsing and bending of the samples are reported also, since these data would be useful in the design and application of the foldable tube for new uses.

DESIGN CONCEPT

The principle upon which the foldable tube is based is that the maximum strain which occurs during collapse is the surface strain resulting from the flattening of a cylindrical section. The tube was geometrically constructed from six cylindrical segments, all with equal radii of curvature (fig. 1). The symmetrical sides were joined by welding at the tangent point; in this case the maximum strain in the weld was thus the result of the force required to bend a 0.020-inch sheet. The centerline of the sheet experienced zero stress, of course, as one side was in compression and the other was in tension. The tension in the weld caused by flattening the tube could be reduced, if necessary, by extending the edges parallel before they are welded; this extension would give the weld a lever arm in bending the sheet and, therefore, reduce the stress.

When a cylindrical section is flattened, the maximum or surface strain ϵ is equal to one-half the thickness t divided by the radius of curvature r; that is, $\epsilon = t/2r$. Therefore, when selecting a material, a high yield point and a low modulus of elasticity are usually desirable in order to maximize the permissible strain, since yield strain is the ratio of yield stress to modulus of elasticity. Selecting a material with these characteristics maximizes the ratio t/r and permits a thicker material or a smaller radius of curvature, whichever is better for the specific application. In some cases, it may be unnecessary to maximize the ratio t/r; material with a low yield strain and high modulus could therefore be used. These elements plus the environment of the tube must be considered in the selection of material for the tube. There are several stainless steels and nickel superalloys which have high yield points and could be used in most applications. In addition, titanium and some hard copper alloys would be very good for many structural uses, as their low moduli of elasticity (approx 15×10^6 compared with approx 29×10^6 for steel) offsets their lower yield points.

The final contour of the tube is determined after the selection of the material on the compatability basis. The minimum material thickness must be consistent with the working pressure or structural strength required. The thickness and the yield strain determine the minimum radius of the contour, since $r = t/2\epsilon$. The required flow area or moment of inertia of the tube in conjunction with the minimum value of r determine the dimensions D and H (defined in fig. 1) or the overall size. The cross-sectional contour for a given flow area was determined graphically by trial and error with the use of only the extended convex arcs to describe the area. This approach was simpler and more conservative, as little additional area is enclosed between the concave portions and the extended convex arcs. With the tube thickness D set, the height H is defined by the tangent points A and B (defined in fig. 1) of the concave arcs. For an optimum design, the concave and the convex arcs should be of equal radius of curvature with all arcs tangent at their junctions.

SPECIMEN FABRICATION

The experimental sections were fabricated from AM-350 stainless-steel sheet, 0.020 inch thick. The sides were formed separately on a power brake and checked against a template. They were then joined by heliarc welding the edges. Plates were welded to the ends of the sections to maintain the tube shape at the ends when the center was collapsed; the transition area was thus forced to occur in the given length. This transition area would be similar to actual use when the ends would be attached to a tube or other restraining structure. The completed sections were double-age hardened as follows: heated and held 1 hour at 1350° F, air cooled to room temperature, heated and held 1 hour at 850° F, and air cooled. This treatment gave a theoretical tensile stress of 206 000 pounds per square inch and a yield stress of 173 000 pounds per square inch.

Care must be given to the forming operation to assure that both sides have the same peripheral length, so that in the collapsed position additional strains will not be introduced by unequal widths of the sides. The forming method used was dictated by reasons of economy and expediency; however, the method was felt to be adequate for testing. Die forming would be a better method, and there is little doubt that the strain resulting from collapse would be less than those measured here.

For applications which would require more strength at the edge welds, the height H could be extended slightly. A seam weld could then be run the length of the piece a short distance from the edge. This weld would be in addition to the edge weld and should increase the strength considerably without affecting the operation of the tube.

Photographs of a sample specimen are presented in figure 2. The cross-sectional contour of the design can be seen in the oblique photographs of figures 2(a) and (b). A demonstration of the tube in the collapsed and bent position is presented in figure 2(c). This photograph illustrates better than words the operation of the foldable tube.

PROCEDURE

Although such a foldable tube was bent numerous times (perhaps 100 times) across a man's knee, a more reproducible and controlled method for bending the tube was used for measurement of strains. The method by which the tube was folded was to apply a compressive force near the center of the section. This force collapsed part of the section into a flat sheet, effectively, so that it could be bent. The test fixture used to accomplish collapse and to control the bending is shown in figure 3. One end of the specimen was clamped to the angle bracket A with C-clamps (not shown). Hydraulic pressure was applied to the double-acting cylinder B. This force was transmitted through the pivot arms C to the vertical rods D, which applied the collapsing load to the specimen. In this case two rods were used on each side, so that the size of the collapsed area would be the same each time and be large enough to accommodate the strain gages. After collapse, a slight bend in the specimen would maintain the position while the bridge structure and the loading mechanism were removed to permit a bend test. The free end of the specimen was rotated to the desired degree of bend and a pin placed in one of the indexing holes located at 15° increments to hold the piece in position.

The location and direction of the principal strains induced by collapsing the section were determined by use of Stresscoat (ref. 1). Before applying the Stresscoat, the sections were vapor blasted and cleaned with acetone. An undercoat thinner was then applied before both sides were sprayed with the coating. After the tube was mounted in the test fixture, a given increment of load was applied and removed. The specimen was then sprayed with "Statiflux" to highlight the cracks, which were marked and photographed. The procedure was repeated with increasing load increments to complete collapse.

A characteristic of Stresscoat is that it will crack only in tension; therefore, it will indicate only tension strains in the material when used as indicated previously. The compression strains were found by loading a clean specimen in the test fixture to a point just below the fully collapsed position and then by applying the coating. This load was then released in increments. Compression strains in the material were then indicated by the tension cracks in the coating, which were marked and photographed for each increment.

Strains resulting from bending the specimen are simple tension (on the outer curvature) and compression (on the inner curvature) strains superimposed on the collapsing strains. They are directed along the length of the section and distributed uniformly across the width. The strains caused by the collapse, however, result in a complex biaxial stress pattern. These complex patterns were defined by the coating so that strain gages could be located and alined to read the maximum principal strains directly.

Metal foil strain gages were mounted on both sides of a specimen of each configuration to measure the surface strains induced by collapsing and bending the tube. The attached gages are shown in figure 4. The sections were collapsed and then bent in 15° increments while the strains were recorded on a strain gage recorder.

DISCUSSION

The results of the strain determination on configuration B (fig. 1(b)) by the use of Stresscoat are presented in figures 5 and 6. Stress patterns in the three configurations tested were nearly identical, as were the patterns on either side of a given specimen. The strain patterns for both tension and compression loads are therefore shown only for one side of specimen B except for the fully collapsed compression strains, where both sides are presented.

The series of photographs presented in figure 5 demonstrates the increasing tension strain as the specimen approached collapse. After each increment of load was applied and released, the areas of cracks for that load were circled so that their growth could be followed. The areas numbered 1 will, in most cases, be the most highly stressed areas in the fully collapsed position. The Stresscoat will, at times, develop random cracks because of temperature effects. This crazing can be seen in the left center of figure 5(b) and should be ignored.

During collapse the strains became very high at localized points, as shown in figure 5(c), where some of the Stresscoat actually spalled off. The highest tension strain areas were, as expected, on the concave portion of the tube. A biaxial strain was present in several areas, as demonstrated by a checkered pattern of cracks.

The compressive strains are illustrated in figure 6. Because of the characteristic of the Stresscoat to crack in tension only, it was necessary to compress the tube to near the collapsed position, to spray with the Stresscoat, and then to remove the load in increments. The resulting cracks then showed the areas that were under compressive strains. Again, the strain cracks were marked as they appeared with each increment of load. The unsymmetrical appearance of figures 6(a) and (b) was created by the difficulty of removing the load uniformly from the two parallel loading bars. The random cracking mentioned previously is again seen on the left in figure 6(b). The highest compressive strain occurred on the convex portion of the tube. In figures 6(c) and (d) the biaxial compressive strain can be seen in a number of places. The lack of Stresscoat in the center was the result of inaccessibility when the coating was applied, not of spalling off.

The radii of curvature obtained by bending the three specimens are shown by line tracings in figure 7. These curves were traced from the edges of the pieces when bent, and the radii were then measured from the paper. There is some variation in curvature between the configurations for each angle of bend, ranging between 1.84 and 2.72 inches ($0.011 > t/r > 0.00735$) at a 90° bend angle. The great flexibility of the tube is demonstrated in figure 7(b) when specimen B was bent nearly 180° with the smallest radius being 0.5 inch ($t/r = 0.04$). In actual use, the tube could be bent around a mandrel to eliminate the very high stresses created by the small radii. These radii indicate that a long tube could be rolled into a coil, if necessary, for a given application.

A presentation of typical strains at the collapsed and at the 90° bend positions are made in figure 8 for each of the three configurations. The location and the orientation of the strain gages are shown with a listing of the strains. The orientations of the gages were determined from the Stresscoat pattern so that the maximum strains could be read directly without the use of strain rosettes, although, as can be seen (fig. 8), some were included. The maximum surface strains measured on collapse were 4500 to 4870 microinches per inch in tension and 4200 to 6200 microinches per inch in compression. Bending the samples increased the maximum strains in both tension and compression to nearly 7000 microinches per inch. Some of these strains are very high and are beyond the straight-line portion of the stress-strain curve for this material (fig. 9) but not beyond the yield point. It should be pointed out that these are surface strains. Ideally, when a cylindrical section of material is flattened or a sheet is bent, the center plane of the material would have zero strain; therefore, if the surface strains should exceed the elastic limit, only a very thin layer of the material would yield. Of course, these strains can be controlled by changing the material thickness or the radii. If the yielded areas remain small, they do not harm the operation of the tube because of the high spring forces of the remaining material.

Since this report is not intended to present a complete stress analysis, table I is included for those interested, but it will not be discussed in detail. It is a tabulation of the measured strains and calculated stresses for pairs of gages alined 90° to each other. The last column is an equivalent stress calculated by the use of Hencky-vonMises theory. The following equations were used for the calculations:

$$\sigma_x = \frac{E}{1 - \mu^2} (\epsilon_x + \mu\epsilon_y)$$

$$\sigma_y = \frac{E}{1 - \mu^2} (\epsilon_y + \mu\epsilon_x)$$

$$\sigma_e = \sqrt{\sigma_x^2 + \sigma_y^2 - \sigma_x\sigma_y}$$

where

σ_x principal stress intensity in x-direction

E modulus of elasticity

μ Poisson's ratio

ϵ_x principal strain in x-direction

ϵ_y principal strain in y-direction

σ_y principal stress intensity in y-direction

σ_e equivalent stress, by Hencky-vonMises yield criterion for plane stresses

The investigation did not include a leak check of the test specimen, a measurement of the rigidity, or extensive quality control of the welds. A visual inspection of the welds made both before and after the tests did not reveal any ruptures. The rigidity of the tube was not tested, but an examination of the cross section indicated that the resistance to buckling from an end load in any direction would be near that of a circular tube with diameter equal to the dimension on the minor axis of the foldable tube.

CONCLUSIONS

Three different configurations of a foldable tube capable of transporting fluids when in the extended position were investigated. They were fabricated from 0.020-inch-thick, AM-350 stainless-steel sheet with contour radii of 2.75 and 4.0 inches. Stresscoat was used to find the location and direction of the maximum tensile and compressive strains, after which strain gages were alined with the principal strains. The maximum measured surface strains were near +4500 and -6000 microinches per inch at the collapsed position. These strains increased to about ±7000, which is still below the yield point, when the specimens were bent 90°. When the tubes were bent after being collapsed, the radii of curvature ranged between 1.84 and 2.72 inches ($0.011 > t/r > 0.00735$ where t is the material thickness and r is the radius of curvature) at a 90° angle. It decreased to 0.5 inch ($t/r \approx 0.04$) at 180° with no apparent damage to the tube.

The foldable tube concept is a practical means for providing a tube that is foldable for launching and, on erection in space, is suitable both for transporting fluid and for providing structural rigidity.

Lewis Research Center,
National Aeronautics and Space Administration,
Cleveland, Ohio, September 17, 1965.

REFERENCE

1. Anon.: Operating Manual for Stresscoat. Magnaflux Corp.

TABLE I. - STRESS-STRAIN READINGS FOR VARIOUS DEGREES OF BEND

Specimen position, deg of bend	First strain gage: Number	First strain gage: Strain, ϵ_x, μin./in.	First strain gage: Stress, σ_x, psi	Second strain gage: Number	Second strain gage: Strain, ϵ_y, μin./in.	Second strain gage: Stress, σ_y, psi	Equivalent stress, σ_e, psi
0(Collapse)	1	368	29.4×10^3	2	1640	64.48×10^3	55.9×10^3
30		-476	+41.04		6080	194.1	177.2
45		-4820	-82.9		8000	216.4	267.7
60		-6300	-134.4		7660	191.5	283.7
75		-6520	-140.5		7780	193.4	290.3
90		-6660	-143.0		8000	199.2	297.7
0(Collapse)	3	-244	34.3	4	4540	146.0	132.2
30		-1150	4.7		4540	137.5	135.2
45		-1650	-7.0		5040	149.2	152.8
60		-2350	-29.5		5080	144.0	160.8
75		-4170	-91.7		4780	117.3	181.4
90		-6000	-154.4		4460	89.8	213.9
0(Collapse)	5	-1460	-60.6	6	-1388	-59.0	59.8
30		-2000	-74.5		-992	-51.0	66.0
45		-3440	-124.6		-1316	-75.1	108.7
60		-3820	-137.3		-1348	79.6	119.4
75		-4150	-147.8		-1316	-81.7	128.2
90		-2820	-103.9		-1268	-67.7	91.3
0(Collapse)	12	4120	130.8	13	-400	25.3	120.2
30		1860	63.2		268	26.1	55.0
45		2550	84.9		180	29.6	74.7
60		2470	83.1		264	31.6	72.7
75		2900	96.8		224	34.3	85.0
90		5540	162.3		-2000	-13.8	169.6
0(Collapse)	18	-3320	-104.7	19	400	-17.8	97.0
30		-2590	-79.4		556	-5.9	76.6
45		-2790	-85.0		660	-4.4	82.8
60		-2830	-85.9		704	-3.3	84.2
75		-2930	-88.7		748	-2.8	87.3
90		-3210	-99.1		616	-9.8	94.6
0(Collapse)	20	8	-19.7	21	-2150	-70.1	62.6
30		76	-14.0		-1772	-57.1	51.5
45		92	-14.8		-1908	-61.5	55.6
60		96	-14.7		-1920	-61.8	55.9
75		76	-15.8		-1960	-63.3	57.1
90		176	-14.4		-2160	-68.9	63.0
0(Collapse)	22	-2110	-95.1	23	-2820	-111.7	104.4
30		368	-2.7		-1584	-48.2	46.9
45		-1040	-56.9		-2470	-90.3	79.1
60		-1160	-61.2		-2510	-92.8	81.7
75		-1644	-78.7		-2700	-103.4	93.5
90		-3920	-156.5		-3060	-136.4	147.5
0(Collapse)	28	796	58.5	29	3490	121.4	105.1
30		2040	94.4		2990	116.6	107.3
45		2670	112.9		2760	115.0	113.9
60		3260	131.9		2730	119.5	126.1
75		4320	166.9		2780	131.0	152.2
90		5280	199.3		2890	143.5	178.1

Specimen position, deg of bend	First strain gage: Number	First strain gage: Strain, ϵ_x, μin./in.	First strain gage: Stress, σ_x, psi	Second strain gage: Number	Second strain gage: Strain, ϵ_y, μin./in.	Second strain gage: Stress, σ_y, psi	Equivalent stress, σ_e, psi
0(Collapse)	30	612	15.5×10^3	31	-484	-10.1×10^3	22.3×10^3
30		-152	-10.7		-616	-21.5	18.6
45		312	-7.6		-1908	-59.5	56.0
60		632	12.6		-868	-22.5	30.7
75		1820	48.2		-1208	-22.6	62.6
90		3410	97.0		-1536	-18.6	107.5
0(Collapse)	32	304	-13.3	33	-2500	-78.8	73.1
30		808	-2.7		-3120	-94.4	93.1
45		876	-4.8		-3590	-109.1	106.8
60		1176	5.0		-3600	-106.6	109.2
75		2040	34.5		-3450	-93.7	114.9
90		3640	88.1		-3300	-73.7	140.5
0(Collapse)	35	-184	-35.4	36	-3160	-104.9	92.4
30		1828	34.4		-2720	-71.8	93.9
45		2630	61.7		-2600	-60.4	105.7
60		2640	61.9		-2610	-60.7	106.1
75		3020	74.6		-2580	-56.1	113.6
90		3290	84.0		-2520	-51.7	118.6
0(Collapse)	39	2630	97.4	40	1240	65.0	65.9
30		3690	159.2		4160	170.2	164.9
45		3680	168.0		5140	202.1	187.4
60		3790	169.0		4860	194.0	182.8
75		3800	167.0		4640	185.6	177.0
90		3870	168.6		4540	184.3	177.0
0(Collapse)	45	124	-20.5	46	2640	-85.1	76.9
30		332	-7.6		-1980	-61.6	58.1
45		336	-7.9		-2030	-63.2	59.6
60		340	-7.7		-2020	-62.8	59.3
75		352	-7.7		-2060	-64.0	60.5
90		368	-----		-----	------	-----
0(Collapse)	47	304	-8.3	48	-1960	-61.2	57.5
30		436	.8		-1440	-43.0	43.4
45		436	.5		-1480	-44.3	44.5
60		444	.7		-1476	-44.2	44.6
75		452	.8		-1496	-44.8	45.2
90		456	.2		-1580	-47.3	47.4
0(Collapse)	50	-1068	-69.4	51	-3700	-130.8	113.3
30		128	-28.7		-3530	-114.1	102.8
45		144	-29.4		-3660	-118.2	106.6
60		144	-29.5		-3680	-118.9	107.2
75		144	-30.7		-3800	-122.7	110.6
90		224	-30.2		-4030	-129.5	117.4
0(Collapse)	67	3290	110.1	68	288	40.0	96.5
30		3680	79.4		-4380	-108.8	163.6
45		3310	57.1		-5480	-148.1	183.5
60		3240	58.0		-5140	-137.7	174.1
75		3240	60.7		-4840	-127.9	166.8
90		3190	59.5		-4800	-127.0	165.0

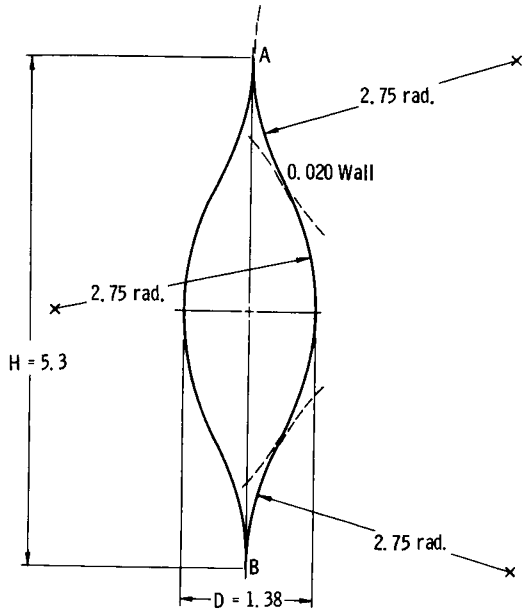

(a) Configuration A. Width, 1.38 inches (equivalent to 2-in.-i.d. tube); cross-sectional area, approximately 3.25 square inches.

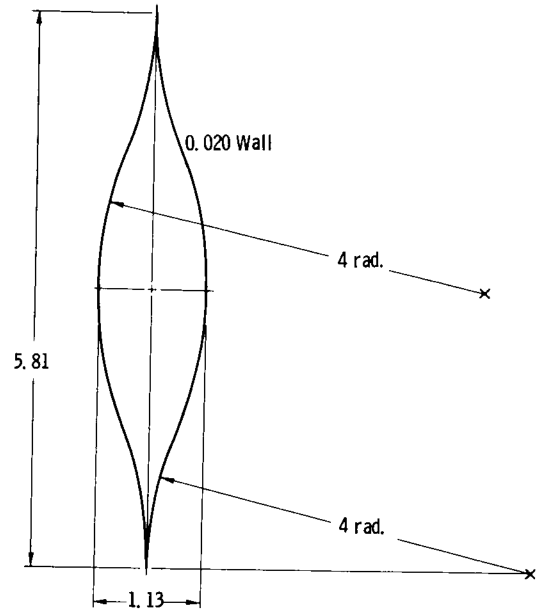

(b) Configuration B. Width, 1.13 inches (equivalent to 2-in.-i.d. tube); cross-sectional area, approximately 3.2 square inches.

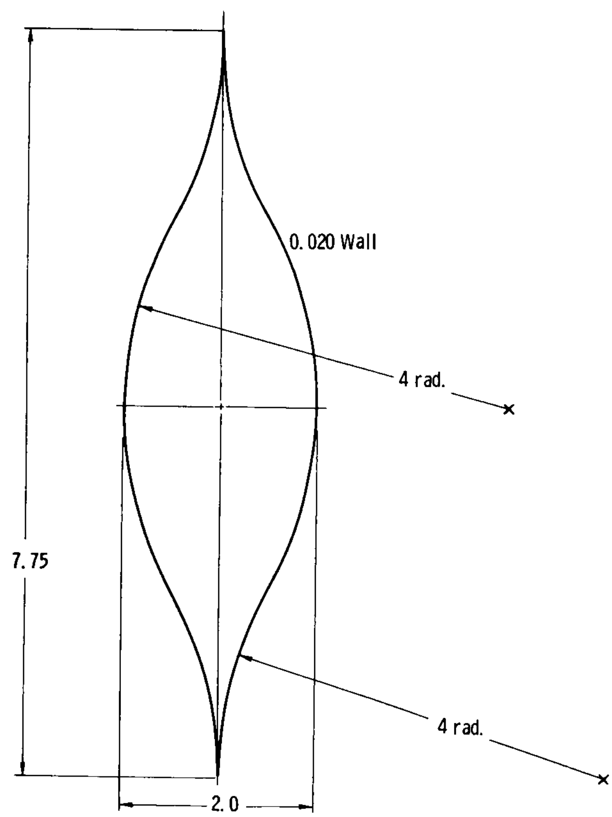

(c) Configuration C. Width, 2.00 inches (equivalent to 3-in.-i.d. tube); cross-sectional area, approximately 4.5 square inches.

Figure 1. - Cross sections of test sections. (All dimensions are in inches.)

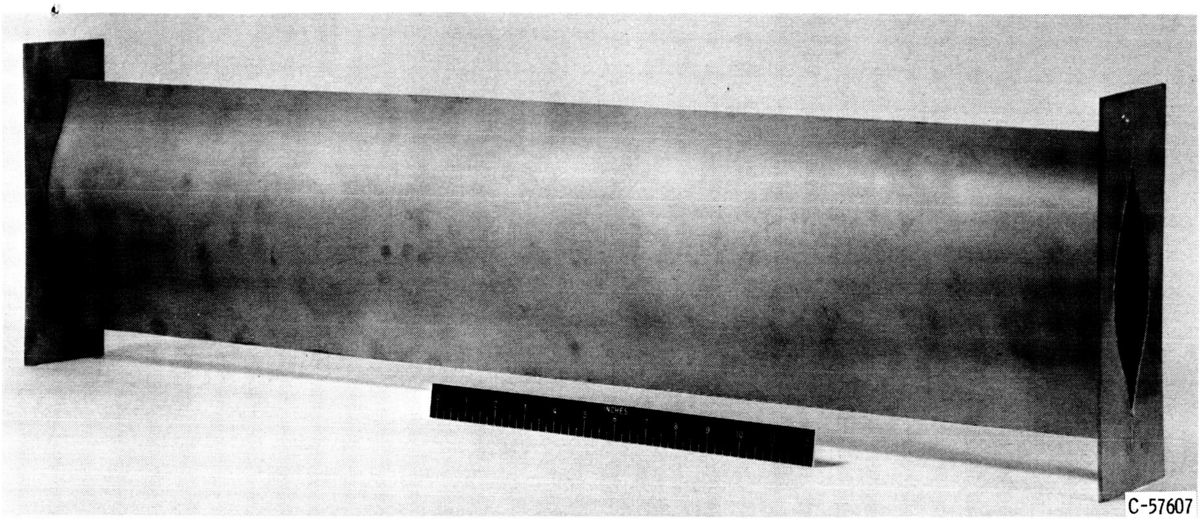

(a) Side view.

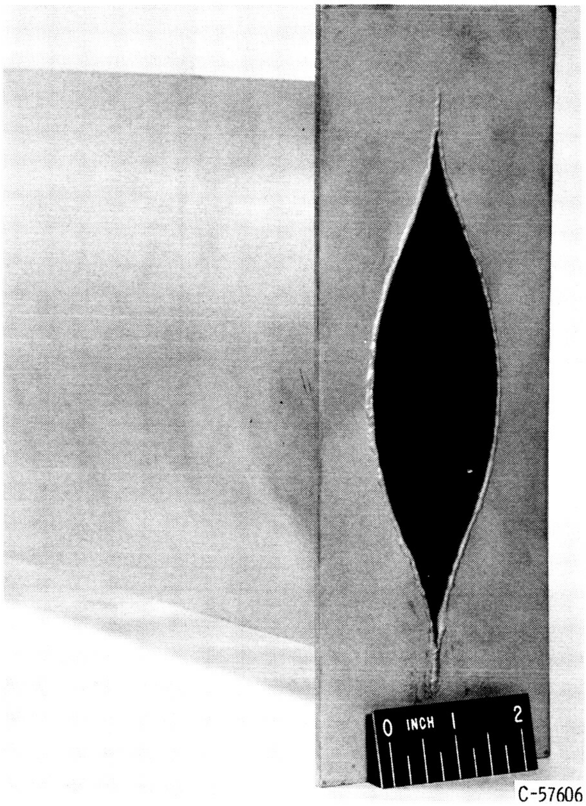

(b) Oblique view of end showing closeup of cross section.

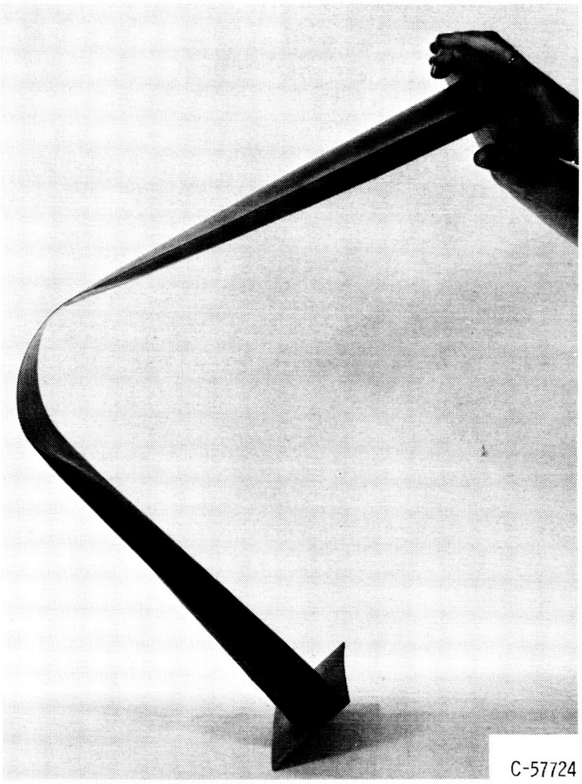

(c) Specimen in collapsed and bent position.

Figure 2. - Foldable-tube specimen equivalent to 3-inch-inside-diameter tube.

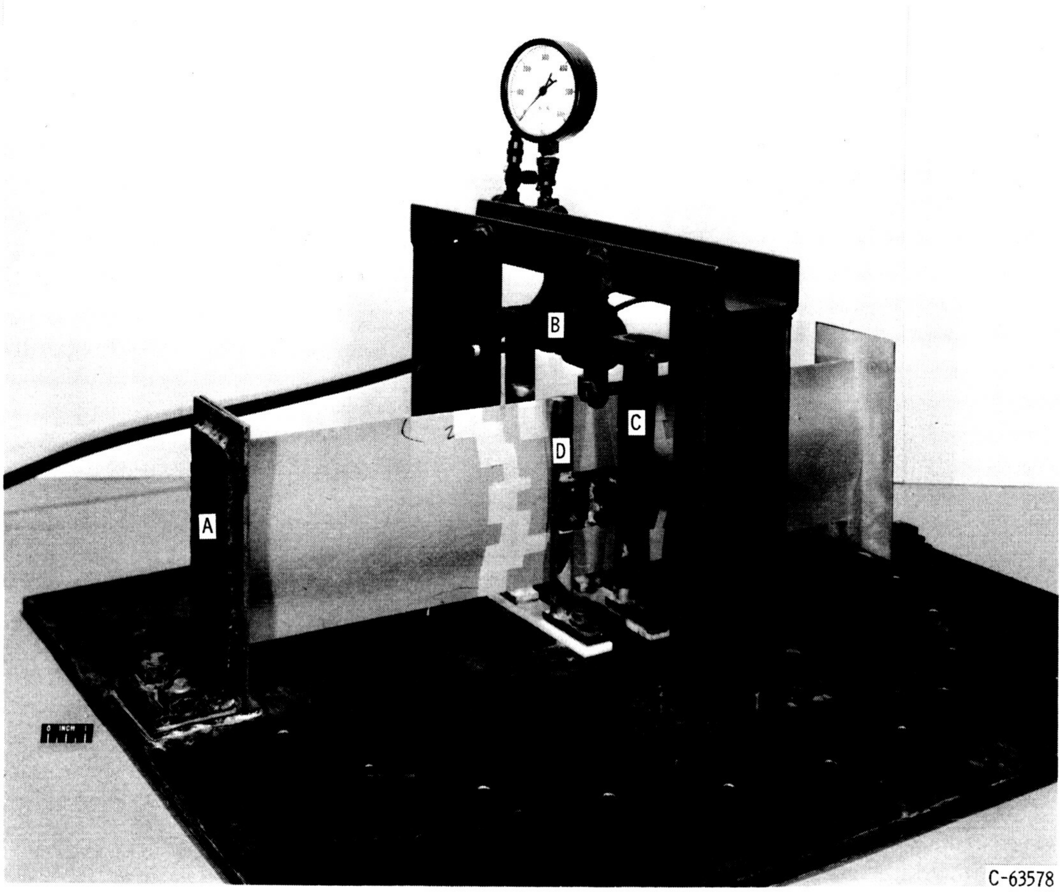

Figure 3. - Rig used to collapse and bend the test piece.

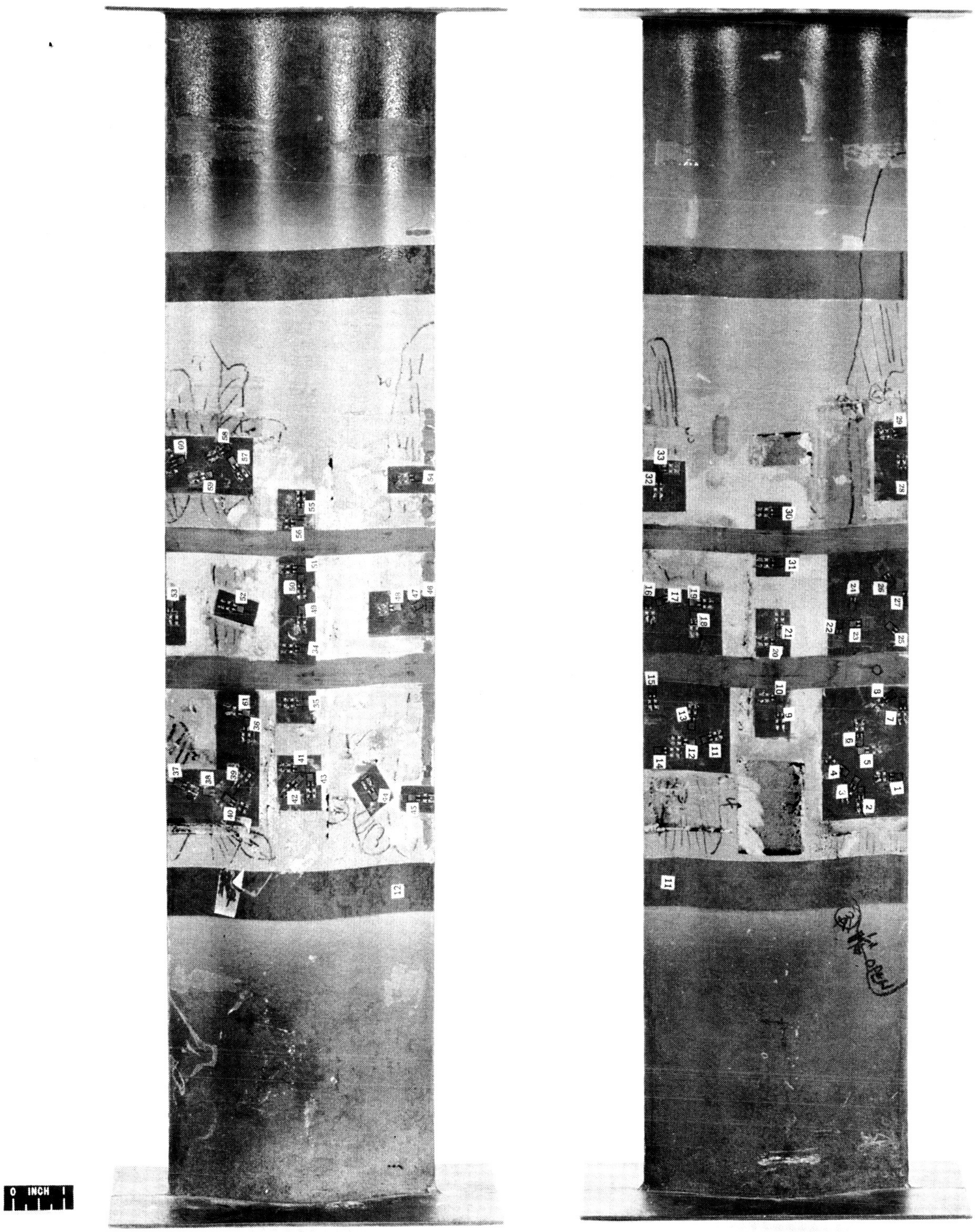

C-65674

(a) Compression side of configuration A.

C-65673

(b) Tension side of configuration A.

Figure 4. - Test specimen with strain gages attached and numbered.

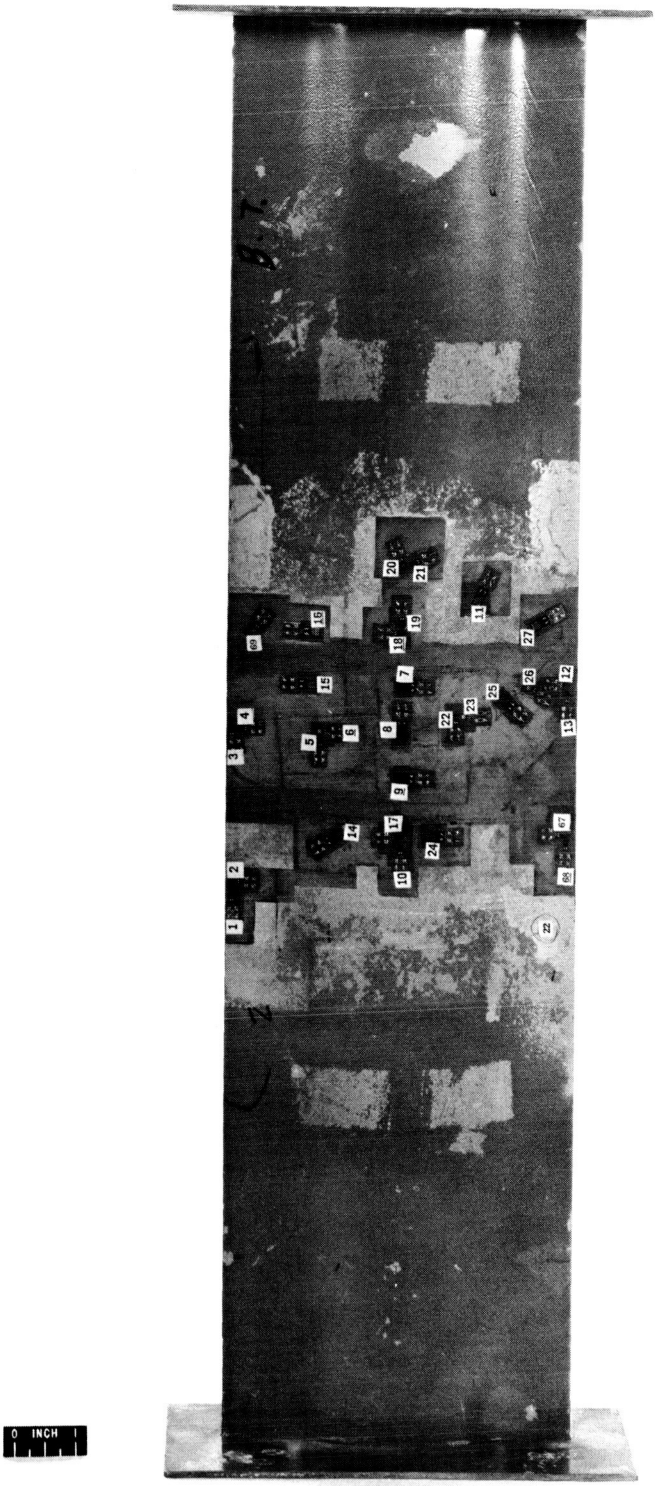

C-65672

(c) Compression side of configuration B.

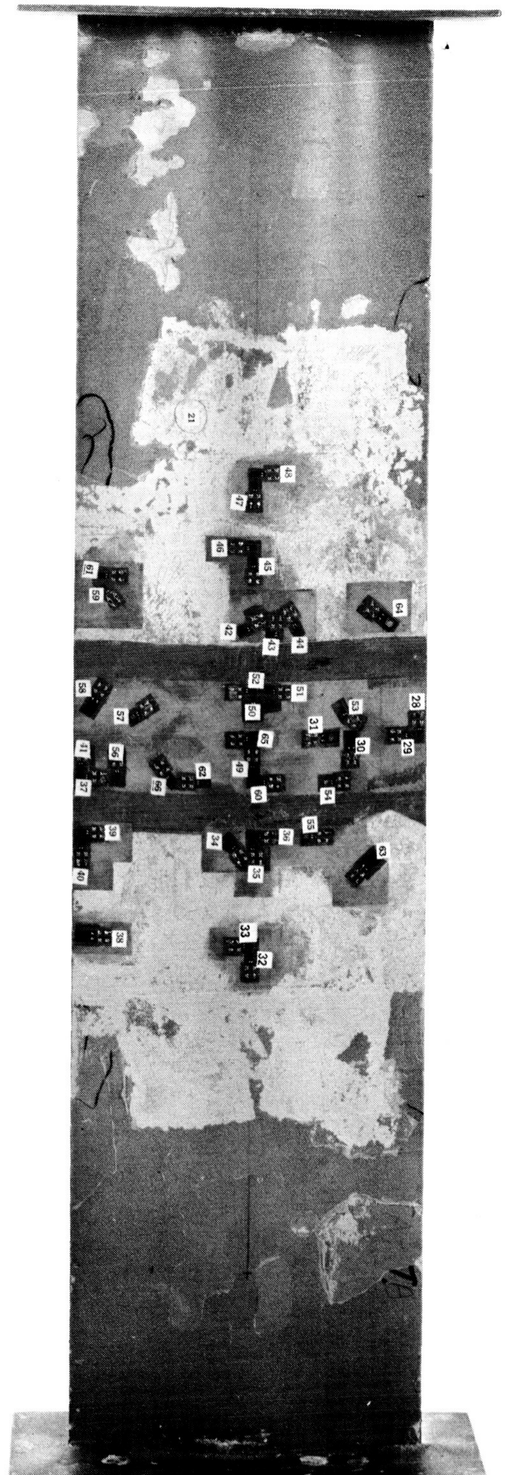

C-65670

(d) Tension side of B.

Figure 4. - Concluded.

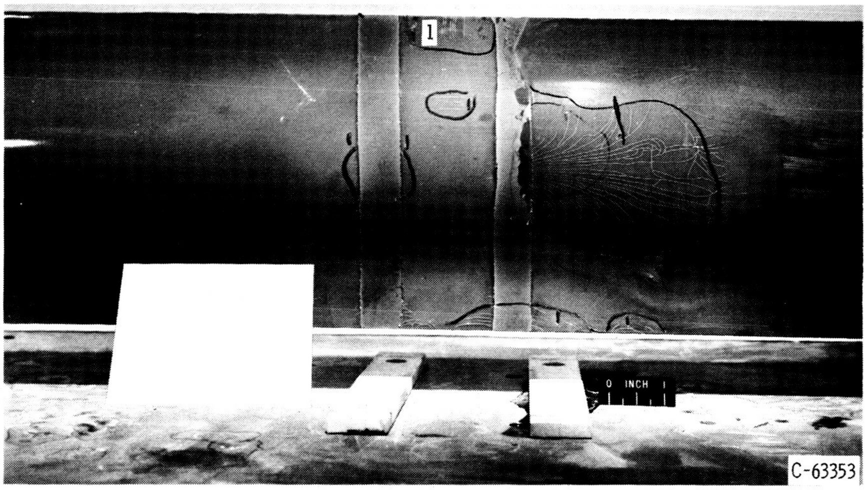

(a) After first increment of load.

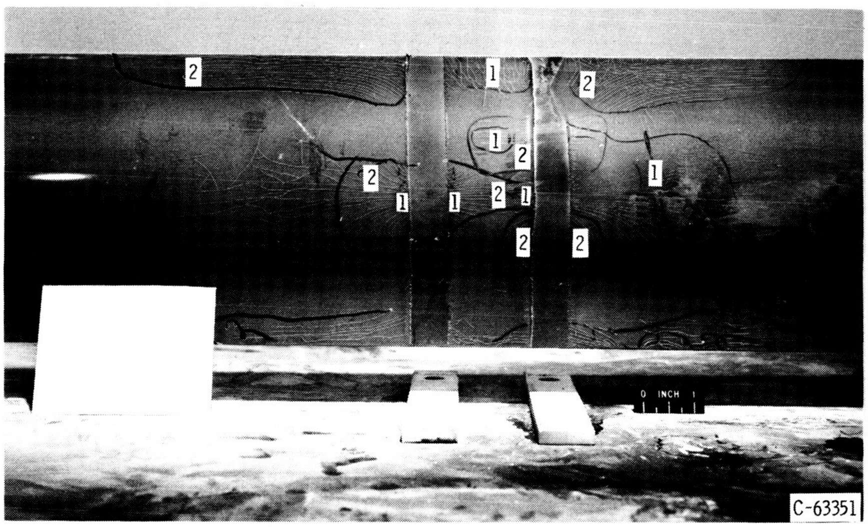

(b) After second increment of load.

(c) After complete collapse.

Figure 5. - Tension cracks in Stresscoat after increments of load were applied to configuration B.

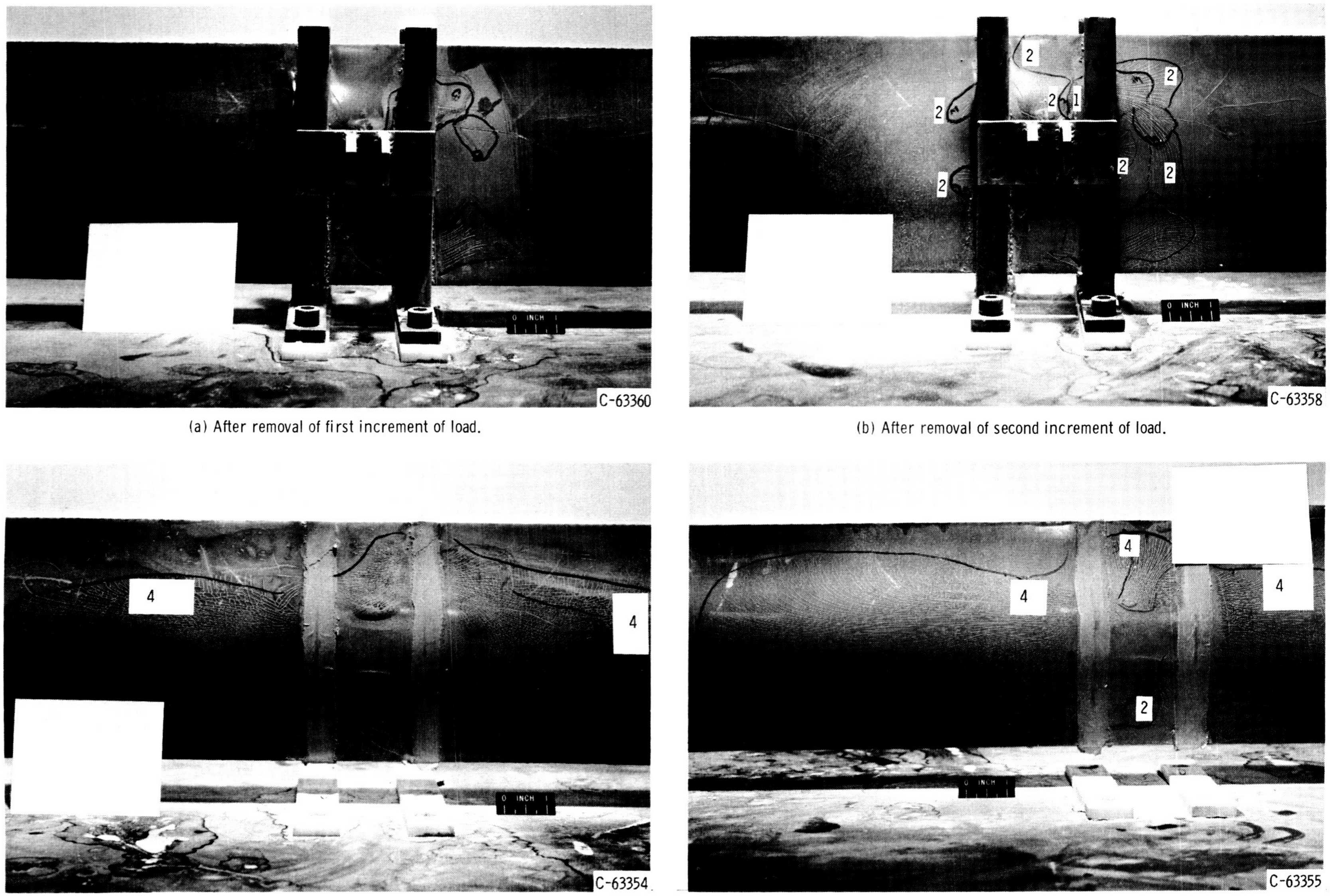

(a) After removal of first increment of load.

(b) After removal of second increment of load.

(c) After complete removal of load, corresponding to collapse.

(d) Back side after complete removal of load.

Figure 6. - Cracks in the stresscoat on configuration B indicating compressive strains formed by starting near the collapsed position and removing load.

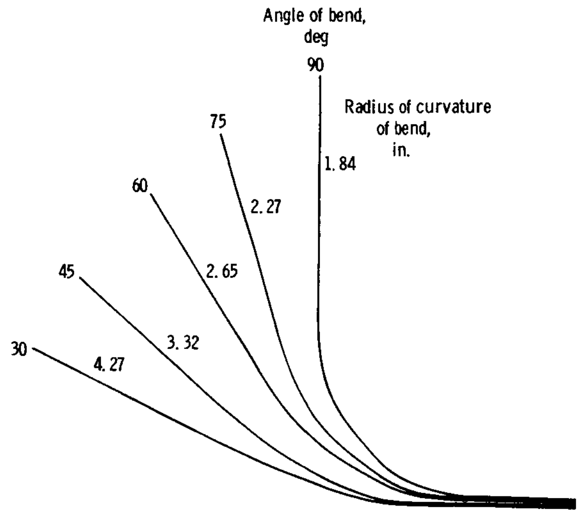

(a) Configuration A. Width, 1.38 inches.

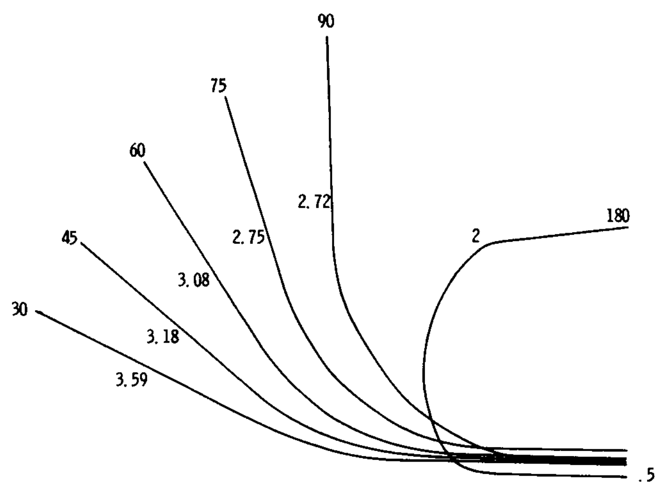

(b) Configuration B. Width, 1.13 inches.

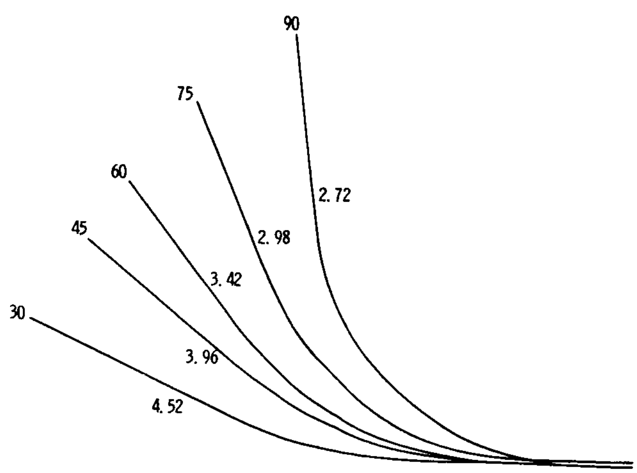

(c) Configuration C. Width, 2.0 inches.

Figure 7. - Tracings of actual curvatures during bending of specimen.

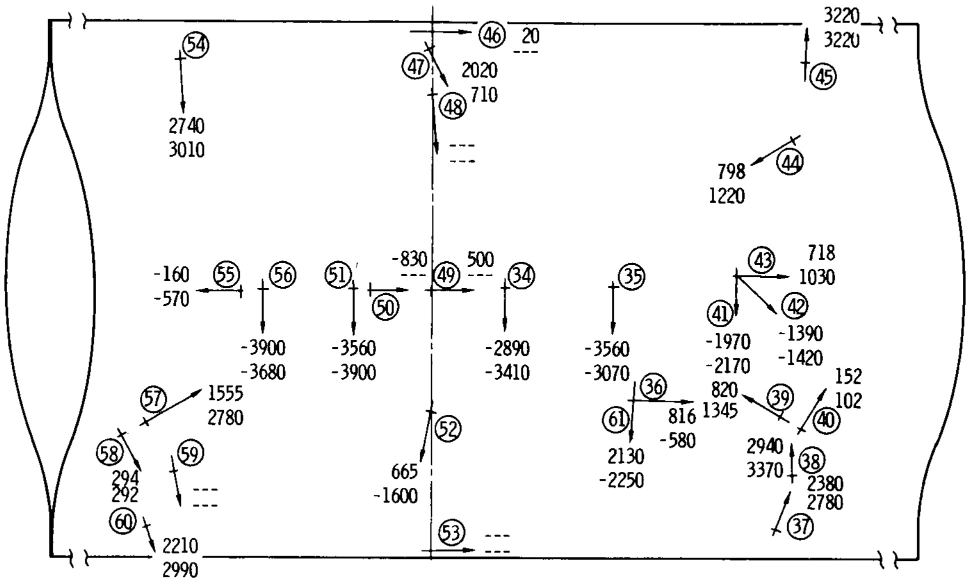

(a) Compression side of configuration A.

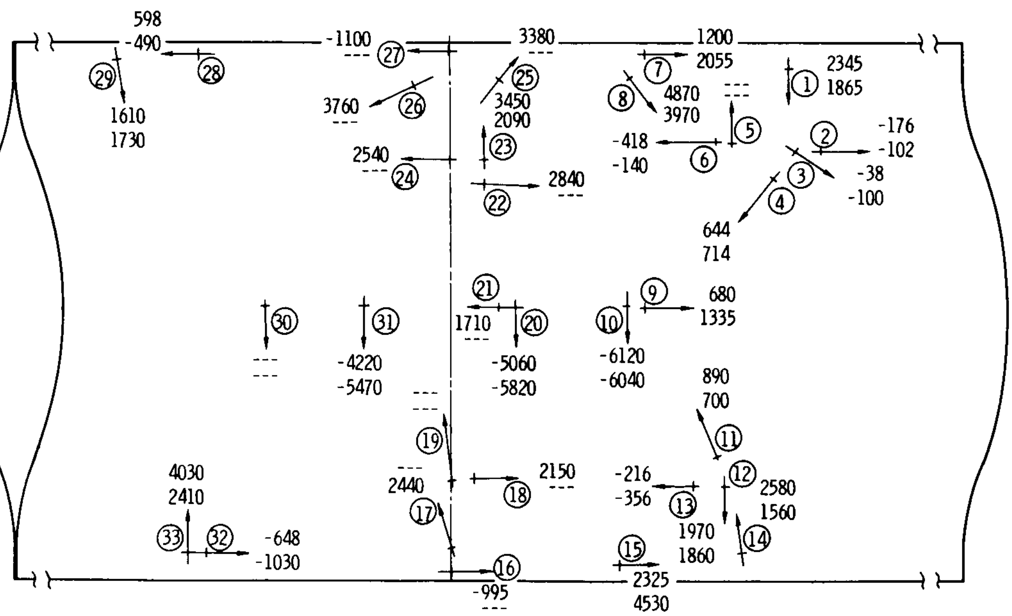

(b) Tension side of configuration A.

Figure 8. - Location, direction, and magnitude of measured strains at the collapsed and the 90° bend position. Circled numbers are strain-gage numbers; strains are in microinches per inch; top number denotes strain at full collapse; bottom number denotes strain at 90° bend.

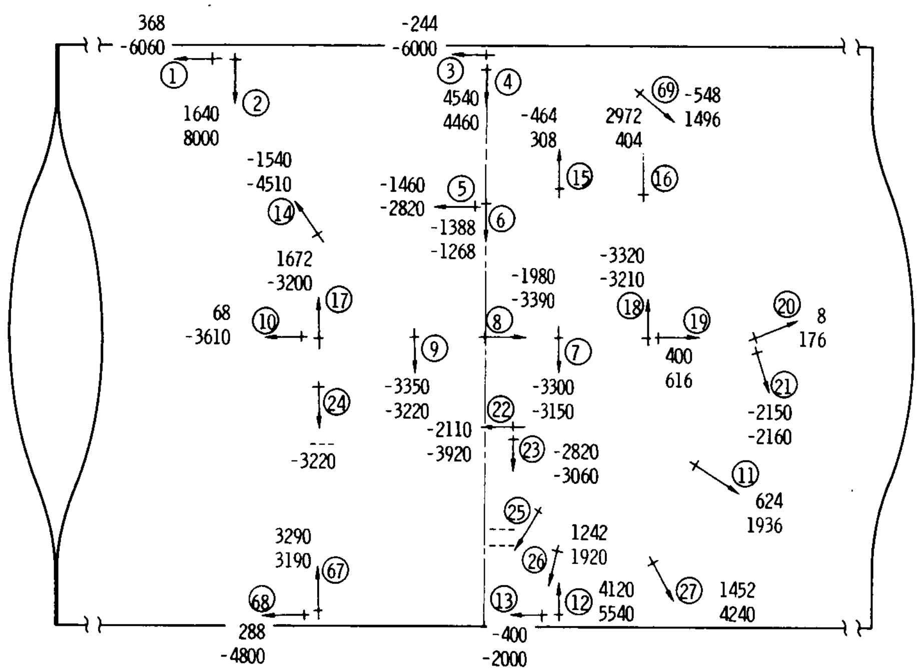

(c) Compression side of configuration B.

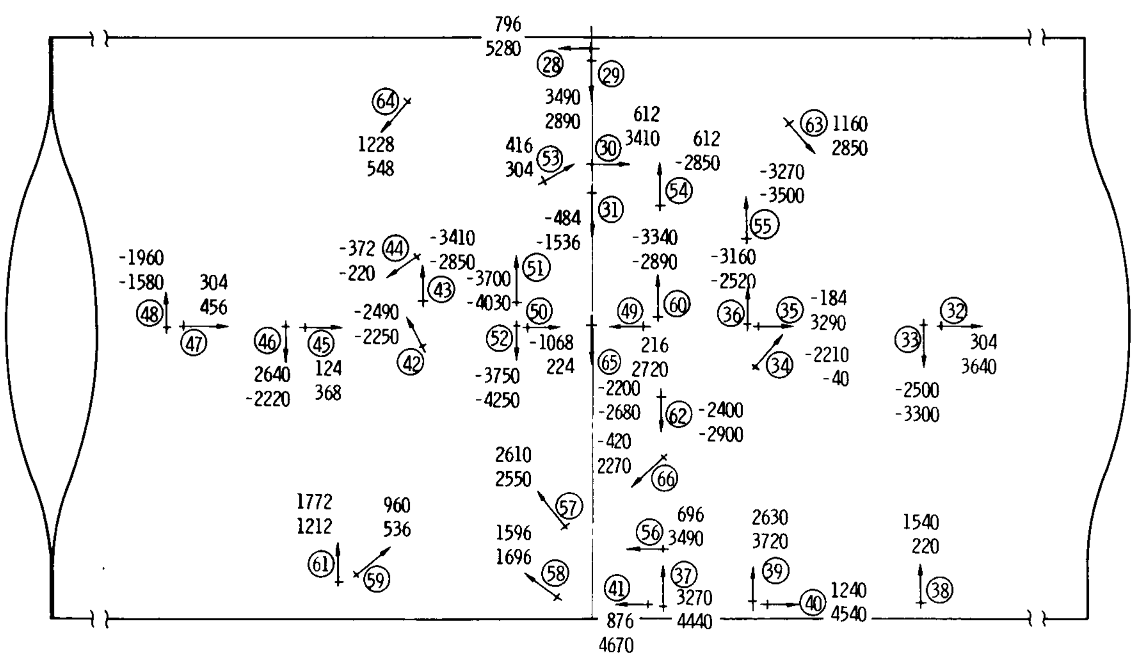

(d) Tension side of configuration B.

Figure 8. - Continued.

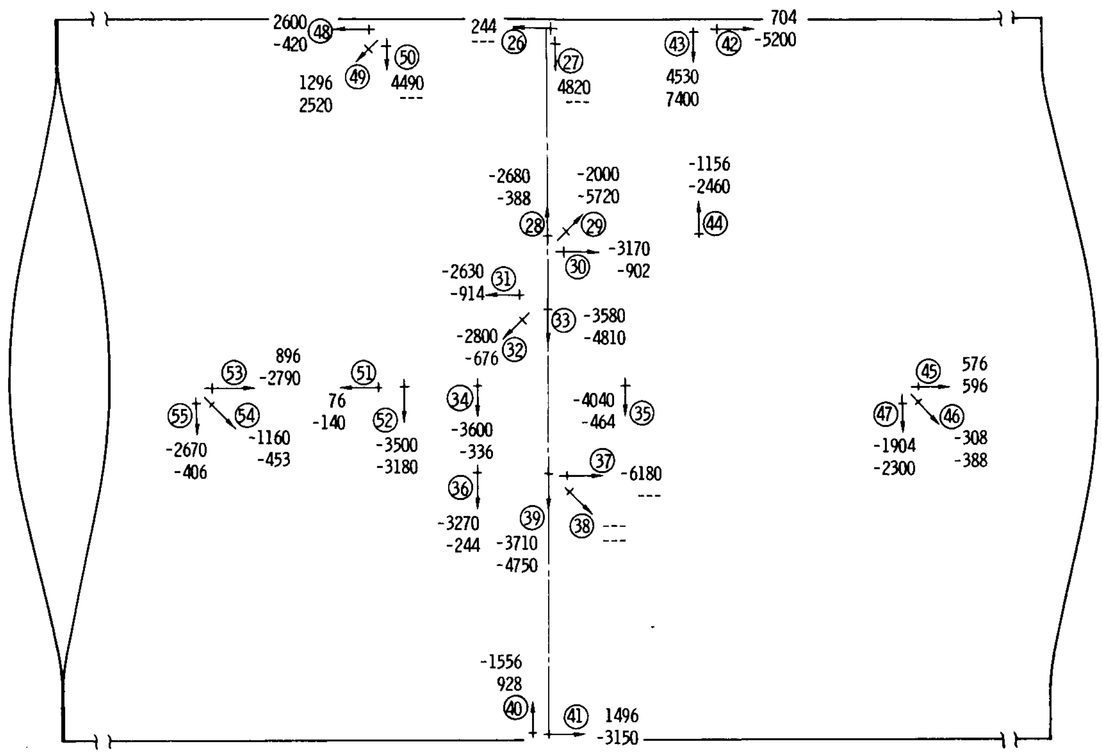

(e) Compression side of configuration C.

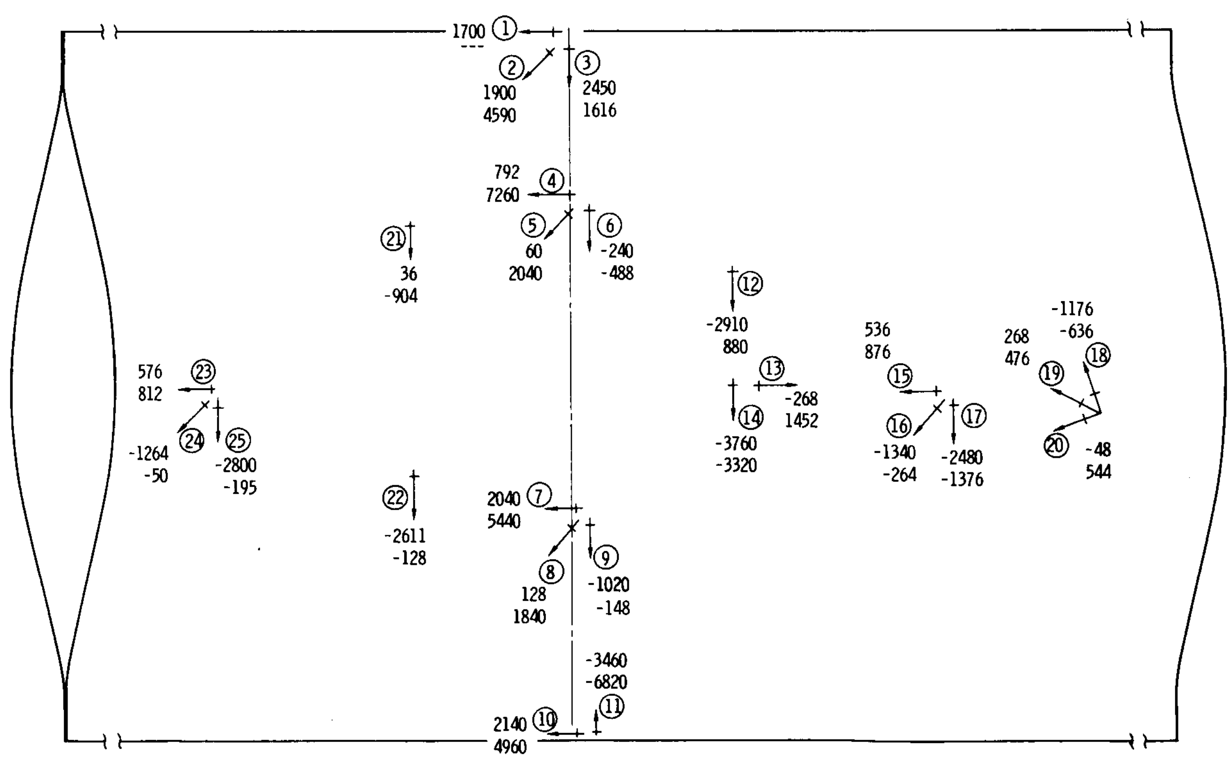

(f) Tension side of configuration C.

Figure 8. - Concluded.

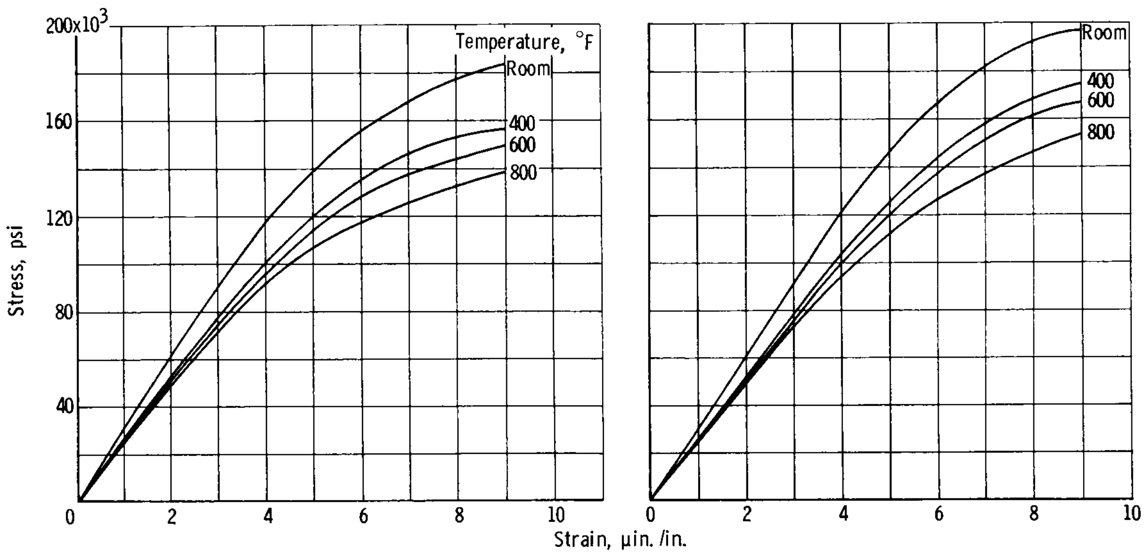

(a) Tensile load.

(b) Compressive load.

Figure 9. - Typical stress-strain curves for AM-350 stainless steel.